Dark conductivity and photoconductivity in solid films of C_{70}, C_{60}, and K_xC_{70}

M. Hosoya, K. Ichimura, Z. H. Wang, G. Dresselhaus, and M. S. Dresselhaus
Massachusetts Institute of Technology, Cambridge, Massachusetts 02139

P. C. Eklund
Department of Physics, University of Kentucky, Lexington, Kentucky 40506
(Received 31 March 1993; revised manuscript received 20 September 1993)

We report the dark conductivity and photoconductivity (σ and $\Delta\sigma$) in sublimed films of C_{70}, C_{60}, and K_xC_{70}. In comparison with C_{60}, the maximum quantum efficiency of C_{70} in air ($\sim 5\times10^{-3}$) is two orders of magnitude higher. The frequency-response range of the photoconductivity of C_{70} is wider than that of C_{60} as well. The disorder and charge localization are important for the charge transport in C_{70}, reflected in a bimolecularlike recombination and a large temperature dependence of the dark conductivity. The Fowler plot suggests that the energy gap of C_{70} is smaller (1.5 eV) than that of C_{60} (1.7 eV). The temperature dependence of $\Delta\sigma$ for C_{70} has a local peak between 260 and 270 K, which is possibly related to the freezing of the orientational disorder in C_{70} below 270 K. The photoconductivity in K_xC_{70} is extremely small, probably due to the charge delocalization which increases the recombination rate.

I. INTRODUCTION

Although some measurements have been reported recently on the dark conductivity and photoconductivity of pristine C_{60} films,[1–4] no experimental studies are available on the electrical conductivity and photoconductivity of pristine C_{70} films. Reported quantum efficiency photoconversion values in C_{60} films are relatively low,[1] approximately on the order of 10^{-4} in vacuum. However, the photoconducting films of polyvinylcarbazole (PVK) doped with fullerenes (a mixture of C_{60} and C_{70}) show a remarkably high xerographic performance, comparable with that of the best photoconductors available commercially to date.[5] In this context, because C_{70} exhibits a higher absorption than C_{60} in the longer wavelength region of the spectrum,[6] C_{70} is expected to show a higher photosensitivity over a wider photo-responsive frequency range than C_{60}, and this frequency range covers, in particular, the technologically important longer wavelength regime.

In this paper, the dark-conductivity and photoconductivity studies in pristine C_{70} and potassium-doped C_{70} (K_xC_{70}) films are reported along with the results for C_{60}. The spectrum of the photoconductive response, as well as the dependence of the photoconductivity on temperature and illumination power, is compared among these three kinds of films. It is revealed that C_{70} films show higher quantum efficiency and a wider spectral sensitivity, as compared with C_{60}. Most of the unusual transport phenomena in C_{70} are attributed to the disorder of the films, which appears to be more pronounced than that of C_{60} films.

II. EXPERIMENTS

Pristine C_{70} and C_{60} films of 2500 Å and 2000 Å thickness, respectively, were deposited on glass substrates over precoated silver electrodes by thermal sublimation of C_{70} and C_{60} powders (Fig. 1). The purity of the powders was at least 96% in C_{70} and 98% in C_{60} by weight. For the conductivity measurements of the pristine films, sandwich cells were constructed by depositing semitransparent aluminum electrodes (200 Å thick) on top of the above mentioned fullerene films. The light transmittance of the top electrodes was 39% at the wavelength of 488 nm. For the measurements of K_xC_{70}, the C_{70} film without any top electrodes was doped with potassium, following the procedure developed by Wang *et al.*[7] The doping was stopped at several different resistances to measure the dark conductivity and the photoconductivity. The higher conductivity of the doped sample allowed measurements to be made between different bottom electrodes. The sample was kept in a glass tube under vacuum during the doping and the subsequent dark-conductivity and photoconductivity measurements. The photoconductivity was measured by a steady-state method, by determining the conductivity in the dark and under illumination and then taking the difference between the two measurements.

III. RESULTS AND DISCUSSION

Conductivity measurements of pristine C_{70} and C_{60} were carried out by applying +1 V to the top semitrans-

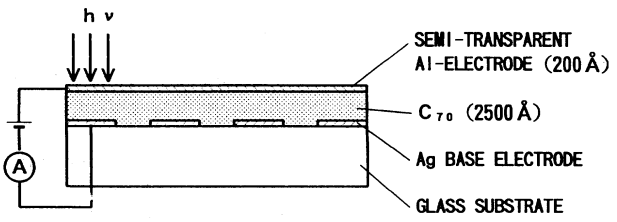

FIG. 1. Configuration of the C_{70} sample.

parent electrodes. Figure 2 shows the relation between the incident light intensity and the photoconductivity, measured in air under illumination by an Ar-ion laser beam of 488 nm. Open circles show the photoconductivity taken just after the deposition of the top electrodes, and full circles show the data taken two weeks after the initial measurements. During the two weeks, the samples were normally kept in the dark in air, but occasionally they were exposed to light for measurements of the action spectrum (photoconductivity versus wavelength) and the temperature dependence of the photoconductivity. Dark-conductivity values, drawn with dashed and solid horizontal lines in Fig. 2, were initially 8.4×10^{-13} $(\Omega\,\mathrm{cm})^{-1}$ in C_{70} and 2.0×10^{-15} $(\Omega\,\mathrm{cm})^{-1}$ in C_{60}, which decreased to 1.5×10^{-13} $(\Omega\,\mathrm{cm})^{-1}$ and to 4.6×10^{-16} $(\Omega\,\mathrm{cm})^{-1}$, respectively, after two weeks. These decreases are considered to be due to the effects of oxygen incorporation[8] and/or the exposure of the films to light. Indeed, the initial dark conductivity of C_{60} increased to 1.8×10^{-14} $(\Omega\,\mathrm{cm})^{-1}$ in a vacuum of 1×10^{-4} Torr, which is in good agreement with the values reported by Mort *et al.*[1] The dark conductivities of C_{70} measured at four positions in two samples were all on the order of 10^{-13} $(\Omega\,\mathrm{cm})^{-1}$ in air. Therefore we can conclude that the dark conductivity of C_{70} is higher than that of C_{60} by two to three orders of magnitude (see Fig. 2).

The photoconductivity of C_{70} is also higher than that of C_{60} by two to three orders of magnitude. The slope of the photoconductivity in Fig. 2 shows different trends between C_{70} and C_{60}. In C_{60}, carrier recombination is dominated by a monomolecular process in the low-light-intensity (low P) regime and by a bimolecular process in the high-light-intensity regime, because the slopes in the $\ln\Delta\sigma$-vs-$\ln P$ plot, labeled as open triangles in Fig. 2, are approximately ~ 1 and ~ 0.6, respectively. This result is qualitatively consistent with the report of Yonehara and Pac.[4] In contrast, the slope values for C_{70} indicate the dominance of a bimolecular process in all light-intensity regimes. This result suggests that in the C_{70} films, carrier recombination takes place between two photoexcited carriers rather than between photocarriers and thermally excited carriers. We note that a bimolecular process normally appears when $\Delta\sigma \gg \sigma$. Hence the appearance of a bimolecular process in C_{70} even for $\Delta\sigma < \sigma$ seems puzzling. The puzzle can, however, be understood in terms of a disordered-solid or a molecular-solid picture for C_{70}. For a disordered solid, charges are well localized. The photoexcited charge carriers Δn have very little opportunity to recombine with the dark carriers n which are located somewhere else, leaving the dominant recombination process to occur among the photocarriers themselves, since they are physically closer to one another. The source of the disorder might be intrinsic disorder effects such as orientational disorder, synthesis-related defects, or extrinsic disorder due to oxidation, impurities, etc. Another feature is the decrease of the slope value Δ in the photoconductivity data during a two week period, which was observed in both C_{60} and C_{70}. This decrease is naturally attributed to the increased disorder due to oxidation on the basis of the disordered-solid picture.

By replotting Fig. 2, the relation between the quantum efficiency, i.e., the number of photogenerated carriers per absorbed photon, and the incident light intensity is obtained (Fig. 3). In this figure, we find a maximum quantum efficiency of 5.2×10^{-3} for C_{70}, which is larger than

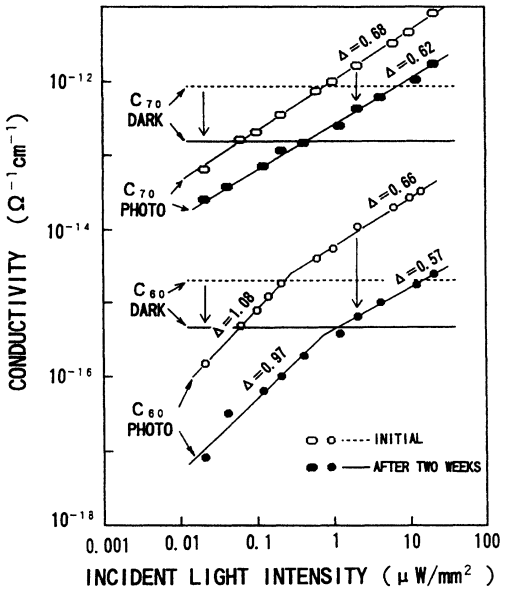

FIG. 2. Incident light-intensity dependence of the photoconductivity in C_{70} (ellipses) and C_{60} (circles), taken in air. Open ellipses and circles show the data taken just after sample preparation, and full ellipses and circles show the data taken two weeks after the initial measurement. Horizontal lines show the dark conductivity for the initial measurements (dashed) and after two weeks (solid). The values of the slopes of these log-log plots for the photoconductivity are shown by $\triangle$. The dark conductivity and photoconductivity in C_{70} are larger than that in C_{60} by about two orders of magnitude.

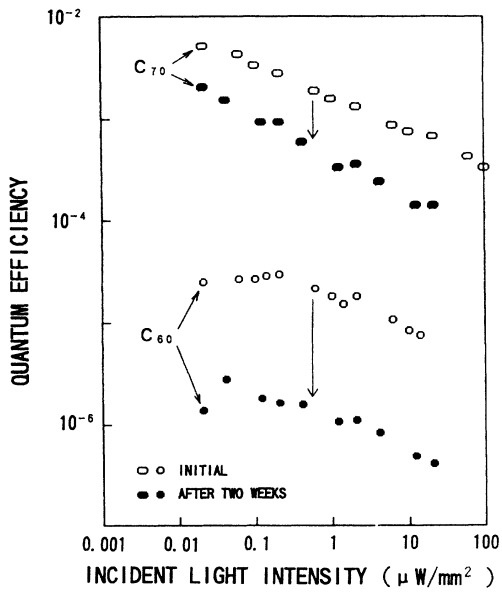

FIG. 3. Quantum efficiency versus incident light intensity, replotted from Fig. 2. The maximum efficiency values are 5.2×10^{-3} in C_{70} and 3.0×10^{-5} in C_{60}. The efficiency for C_{60} increased up to 1.2×10^{-4} in vacuum.

that of C_{60} ($\sim 2 \times 10^{-5}$) by two orders of magnitude. In C_{60}, the quantum efficiency is approximately constant at low light intensities and decreases at higher intensities. These trends can be explained in terms of the formula

$$\Delta n = \frac{g}{2C_n n_0} \tag{1}$$

for a monomolecular process and

$$\Delta n = \left(\frac{g}{C_n}\right)^{1/2} \tag{2}$$

for a bimolecular process,[9] where Δn is the number of photoexcited excess carriers, n_0 the density of thermal carriers, C_n the capture coefficient by recombination, and g the carrier generation rate. Because the quantum efficiency η is given by

$$\eta = \Delta n / n_p, \tag{3}$$

where n_p is the absorbed photon number which is proportional to g, η becomes constant in a monomolecular process and proportional to $n_p^{-1/2}$ in a bimolecular process. Furthermore, we found the quantum efficiency of C_{60} in vacuum to be 1.2×10^{-4} at 0.2 μW/mm^2, which is in good agreement with the results of Mort *et al.*[1] In contrast, the quantum efficiency in C_{70} decreases monotonically with increasing power level, indicative of a higher quantum efficiency at light intensities lower than 0.02 μW/mm^2.

Figure 4 shows the photoconductivity action spectra for both C_{70} and C_{60}. The measured photoconductivity was corrected for the spectral response of the light source and monochromator, and the data are normalized to an incident light intensity of 0.2 μW/mm^2. The action spectrum in C_{60} shown here is similar to the results obtained by Yonehara and Pac.[4] Especially the wavelengths for the peak (475 nm) and for the shoulder (600 nm) are in good accord with their results. The spectral shape of the photoconductivity data for C_{70} resembles that in C_{60} and the wavelength for the maximum sensitivity is exactly the same (475 nm). However, the photoconductivity in C_{70} is higher by three to four orders of magnitude than that in C_{60} and the range of sensitivity is extended to the technologically important longer wavelength regime. Indeed, the shoulder is extended to 650 nm and the decrease of sensitivity is much smaller than that in C_{60} in the range above 700 nm.

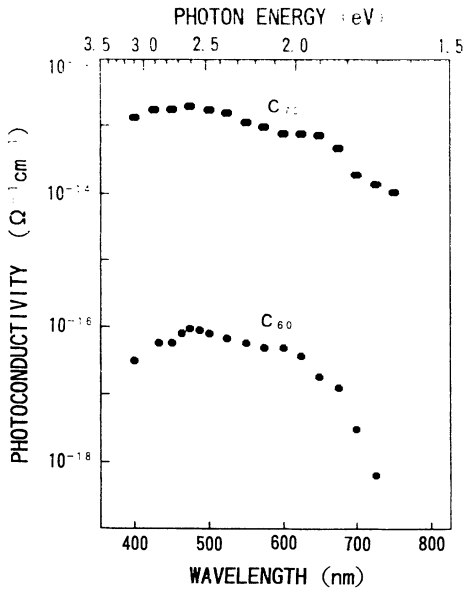

FIG. 4. Action spectrum of the photoconductivity for C_{60} and C_{70} in air, plotted in terms of both wavelength and photon energy. The maximum photoconductivity values are given at 475 nm in both C_{60} and C_{70}. Higher photoconductivity and extended spectral response, especially at longer wavelength, were observed in C_{70}.

When the data are replotted on a Fowler plot, i.e., (quantum efficiency)$^{1/2}$ versus photon energy (Fig. 5), a straight line is obtained below 2.1 eV in C_{60}. From the intercept on the abscissa of the extrapolated linear region, a value of 1.7 eV is obtained for the energy gap of C_{60}, which is in good accord with the reported experimental values of the energy gap.[3,10] In C_{70}, although we cannot find a well-defined straight portion, both the data points between 1.8 eV and 2.5 eV and the tail below 1.8 eV can be extrapolated to the same energy of $\sim$1.5 eV, which corresponds to the energy gap of C_{70}. Therefore the energy gap of C_{70} is smaller than that in C_{60} by 0.2 eV. This result is consistent with the fact that C_{70} shows higher absorption and higher photoconductivity in the longer wavelength region of the spectrum, and also with the theoretical and experimental results in some references[11–13] where the HOMO-LUMO gap of a C_{70} molecule is found to be smaller than that of a C_{60} molecule. Here HOMO and LUMO refer, respectively, to the highest occupied molecular orbital and the lowest unoccupied molecular orbital.

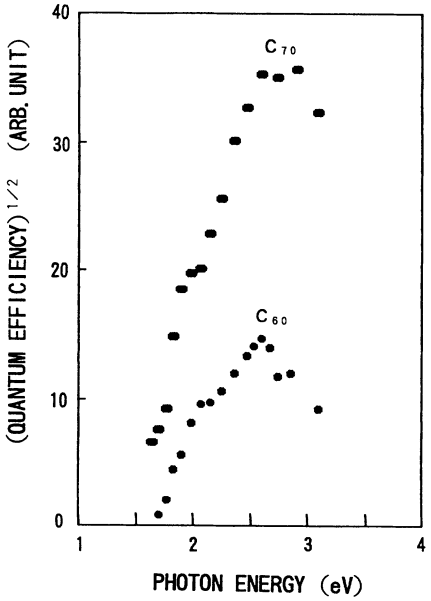

FIG. 5. Fowler-type plots of (quantum efficiency)$^{1/2}$ versus photon energy for C_{60} and C_{70}. The intercepts on the abscissa of the extrapolated linear region indicate an energy gap of 1.7 eV in C_{60} and 1.5 eV in C_{70}.

The temperature dependence of the dark conductivity and photoconductivity was measured in vacuum (50 mTorr residual gas pressure) with an Ar-ion laser of 2 μW/mm^2 light intensity at 488 nm (Fig. 6). Below 230 K in C_{60} and below 200 K in C_{70}, the dark currents became dominated by noise. The values of σ and $\Delta\sigma$ in vacuum were larger than those in air in C_{60}, although little difference was observed in C_{70}. The dark conductivity (full circles) shows a linear dependence on $1000/T$ at high temperatures in C_{60}. It has been reported that the dark conductivity of C_{60} exhibits a maximum at about 250 K, which was proposed to be connected with the orientational phase transition at 249 K.[14–16] There is, however, no local maximum in our result. This discrepancy is possibly attributed to a lack of preannealing of the samples over 400 K prior to the experiments. Indeed, it has been demonstrated that the magnitude of the local maximum structure is dependent on the thermal history of the sample and that the structure connected with the phase transition is not detectable in samples without preannealing.[2,3]

In contrast, the photoconductivity of C_{70} presents a local peak in temperature between 260 K and 270 K. This peak appears with complete reproducibility, regardless of whether the temperature is increased or decreased in the measurement, although the sample dependence was not fully confirmed. This phenomenon is possibly related to the reported orientational freezing of the C_{70} molecules below 270 K.[17,18] Another feature is the weak temperature dependence of the photoconductivity in C_{70} at low temperatures below the point at which the dark conductivity and photoconductivity cross in Fig. 6. It is not clear if this phenomenon should be attributed to the hopping conduction at low temperatures or to some other mechanism. The temperature dependence of the photoconductivity in C_{60} showed the same trend as that in the previously reported results,[2] where the photoconductivity increased monotonically but nonlinearly with the temperature.

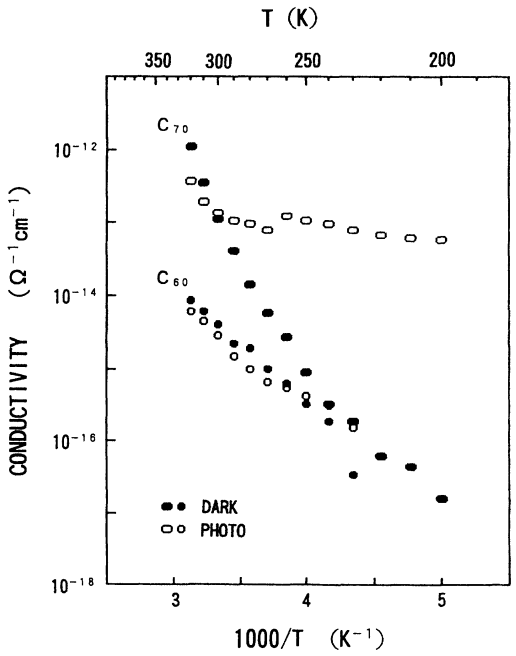

FIG. 6. Temperature dependence of the dark conductivity and photoconductivity for C_{60} and C_{70}, taken in vacuum with a 488 nm Ar-ion laser and an intensity of 2 μW/mm^2. The activation energy value E_a, obtained by the fit at high temperatures, is 0.82 eV in C_{60}. The local peak between 260 K and 270 K in C_{70} may be related to the reported orientational freezing of the C_{70} molecule below 270 K (Refs. 17 and 18).

The activation energy obtained by a fit to the high-temperature data is 0.82 eV for C_{60}, which is about half the energy gap value of 1.63 eV. On the other hand, in C_{70} two different features are found. One is the large values of the activation energy (up to 1.8 eV above 270 K and 1.6 eV between 240 K and 270 K). This activation energy is much larger than the known band-gap value of C_{70} ($\sim$ 1.3–1.5 eV). In the case of a crystal solid, the conductivity is determined by thermal excitation of charge carriers over the energy gap and the activation energy should be approximately half of the value of the band gap. In the disordered solid, however, the σ is dominated by the hopping conduction where the activation energy is determined by a potential barrier describing the disorder. Bearing this in mind, we can see that C_{60} can be reasonably described by a band picture, whereas C_{70} can only be considered as a disordered solid whose potential barrier for the disorder is $\sim 1.6 - 1.8$ eV, which exceeds the band-gap value. In the latter case, charges are well localized due to Anderson localization. Also contributing to the charge localization is the molecular-solid nature of C_{70}. It is likely that both the structural disorder and the molecular-solid nature of C_{70} contribute to charge localization in this material. As mentioned above, the charge localization is the key factor responsible for the observed bimolecular process in C_{70} even for $\Delta\sigma < \sigma$.

The decay time measurements of the photoconductivity suggest that the population of the defect states in the band gap is smaller in C_{70} than in C_{60}, because the half decay times are far smaller in C_{70} than in C_{60}: 0.2 sec at 300 K and 0.3 sec at 200 K in C_{70} as compared to 4 sec at 300 K and 15 sec at 210 K in C_{60}. Long decay times ranging from seconds to days were previously observed in some photoconductors, such as, for example, a-Si:H,[19] GaAs,[20] and disordered carbon materials.[21,22] These phenomena are explained by polaronic states associated with captured carriers at dangling bonds.[19–22] Therefore the longer decay time in C_{60} suggests a higher population of dangling bonds in our C_{60} films. This idea is consistent with the carrier recombination process discussed in connection with Fig. 2. Further experiments, however, may be needed to confirm whether this high population of dangling bonds in C_{60} films is universal or dependent on the sample preparation and/or other factors such as oxygen uptake by the sample.

Finally, Fig. 7 shows the temperature dependence of the photoconductivity for a potassium-doped C_{70} film with a room-temperature dark conductivity of 8.4 S/cm. The measurements were carried out under a constant current of 1 A between two silver electrodes with a gap of 1 mm, on which a C_{70} film was deposited without the top semitransparent electrode. Doping was stopped at three different conductivity values of 40, 8.4, and 1.5 S/cm (at

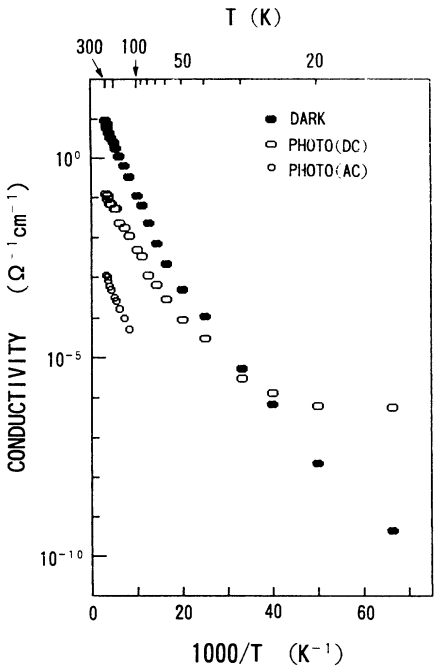

FIG. 7. Temperature dependence of the dark conductivity and photoconductivity for K_xC_{70} in vacuum. The energy of the Ar-ion laser at the sample surface was 200 times that for the measurements on pristine samples in Fig. 6. The activation energy is 55 meV for the dark conductivity. Open circles show the photoconductivity taken with an optical chopper of 50 Hz and a 50% duty cycle and using a lock-in amplifier. The photoconductivity/dark-conductivity ratio at room temperature is much smaller than that in pristine C_{70}.

300 K) in order to measure the temperature dependence at each doping level. Similar to C_{70}, an activation behavior of the dark conductivity at high temperatures and an almost-constant photoconductivity at low temperatures are also observed in K_xC_{70}. However, the magnitude of the photoconductivity for K_xC_{70} is much smaller than that of the dark conductivity (approximately two orders of magnitude smaller at room temperature), even under an illumination of 400 μW/mm^2 which is 200 times greater than the illumination intensity used for the measurement of pristine C_{70}. There are no peaks in the photoconductivity in K_xC_{70} (Fig. 7). The activation energy E_a of the dark conductivity at high temperature decreased with an increase of the room-temperature conductivity, that is, E_a = 77 meV, 55 meV, and 10 meV for samples with conductivity values of 1.5, 8.4, and 40 S/cm, respectively.

It should be noted that the sample heating by the illumination (in Fig. 7) is negligible because the ac photoconductivity (open circles), measured with an optical chopper of 50 Hz and 50% duty cycle and a lock-in amplifier, showed the same trends as that in the dc photoconductivity. The activation energy values for the dark conductivity and ac photoconductivity are almost the same, although that of the dc photoconductivity is smaller. This discrepancy is attributed to the temperature dependence of the rise time of the photoconductivity, which became longer at low temperatures, causing a steeper decrease of the ac photoconductivity. At higher temperatures, the activation energy value for the dc conductivity is expected to approach the same value as that for the dark conductivity and ac photoconductivity.

IV. SUMMARY

In summary, this study reveals a higher photoconductive response in C_{70} films than that in C_{60}. The quantum efficiency of C_{70} in air was as high as 5.2×10^{-3}, higher than that of C_{60} by two to three orders of magnitude. In the action spectra, C_{70} exhibits a maximum photoconductivity response at the same wavelength as that in C_{60} (around 475 nm), although the magnitude of the photoconductivity in C_{70} is larger by three orders of magnitude and the response range for C_{70} also extends to a longer wavelength. The Fowler-type plots of (quantum efficiency)$^{1/2}$ versus photon energy revealed that the energy gap is 1.5 eV in C_{70} and 1.7 eV in C_{60}. A local maximum in the temperature dependence of the photoconductivity between 260 K and 270 K may be related to the reported orientational freezing of C_{70} molecules. The dark conductivity of C_{70} is 10^{-13} S/cm, higher than that of C_{60} by two orders of magnitude. Measurements on K_xC_{70} show a similar trend in the temperature dependence of the dark conductivity and photoconductivity as that in C_{70}, although the photoconductivity for K_xC_{70} at room temperature is much smaller than the dark conductivity. The bimolecular recombination and large thermal activation energy in C_{70} suggest that C_{70} is a disordered solid, or a molecular solid where charges are well localized so that hopping is the dominating transport mechanism.

The results of this study suggest that C_{70} based films have significant potential for application as sensitive photoconductors in technologies like xerography.

ACKNOWLEDGMENTS

We are grateful to Professor R. Saito for helpful discussions and comments. We acknowledge the assistance of K. A. Wang, W. T. Lee, and G. Reynolds. The research is supported by NSF Grant No. DMR-92-01878 and the Toshiba Corporation.

[1] J. Mort *et al.*, Chem. Phys. Lett. **186**, 284 (1991).
[2] J. Mort *et al.*, Appl. Phys. Lett. **60**, 1735 (1992).
[3] M. Kaiser *et al.*, Solid State Commun. **81**, 261 (1992).
[4] H. Yonehara and C. Pac, Appl. Phys. Lett. **61**, 575 (1992).
[5] Y. Wang, Nature (London) **356**, 585 (1992).
[6] M. J. Rosker *et al.*, Chem. Phys. Lett. **195**, 427 (1992).
[7] Z. H. Wang *et al.*, Phys. Rev. B **48**, 16 881 (1993).
[8] H. Werner *et al.*, Angew. Chem. Int. Ed. Eng. **31**, 868 (1992).
[9] *Amorphous Semiconductors*, edited by M. H. Brodsky, Top-

ics in Applied Physics Vol. 36 (Springer-Verlag, Berlin, 1985).
[10] A. Skumanuch, Chem. Phys. Lett. **182**, 486 (1991).
[11] S. Saito and A. Oshiyama, Phys. Rev. Lett. **66**, 2637 (1991).
[12] S. Saito and A. Oshiyama, Phys. Rev. B **44**, 11 532 (1991).
[13] R. E. Haufler *et al.*, Chem. Phys. Lett. **179**, 449 (1991).
[14] J. Mort *et al.*, Chem. Phys. Lett. **186**, 284 (1991).
[15] P. A. Heiney *et al.*, Phys. Rev. Lett. **66**, 2911 (1991); see also Comment by R. Sachidanandam and A. B. Harris, *ibid.* **67**, 1467 (1991).
[16] V. S. Babu and M. S. Seehra, Chem. Phys. Lett. **196**, 569 (1992).
[17] M. A. Verheijen *et al.*, Chem. Phys. **166**, 287 (1992).
[18] G. B. Vaughan *et al.*, Science **254**, 1350 (1991).
[19] J. Kakalios and H. Fritzsche, Phys. Rev. Lett. **53**, 1602 (1984).
[20] D. V. Lang and R. A. Logan, Phys. Rev. Lett. **39**, 635 (1977).
[21] K. Kuriyama and M. S. Dresselhaus, Phys. Rev. B **44**, 8256 (1991).
[22] M. Hosoya *et al.*, J. Mater. Res. **8**, 811 (1993).